Agricultural and Forest Meteorology 232 (2017) 349–358

Contents lists available at ScienceDirect

Agricultural and Forest Meteorology

journal homepage: www.elsevier.com/locate/agrformet

Measurements of methane emissions from a beef cattle feedlot using the eddy covariance technique

Prajaya Prajapati, Eduardo A. Santos*

Department of Agronomy, Kansas State University, United States

ARTICLE INFO

Article history:
Received 20 April 2016
Received in revised form 3 September 2016
Accepted 8 September 2016

Keywords:
Methane emissions
Eddy covariance
Enteric fermentation
Feedlot
Livestock

ABSTRACT

The eddy covariance (EC) technique has been extensively used in several sites around the world to measure energy fluxes and CO_2 exchange at the ecosystem scale. Recent advances in optical sensors have allowed the use of the EC approach to measure other trace gases (e.g. CH_4, NH_3 and N_2O), which has expanded the use of eddy covariance for other applications, including measuring gas emissions from livestock production systems. The main objectives of this study were to assess the performance of a closed-path EC system for measuring CH_4, CO_2, and H_2O fluxes in a beef cattle feedlot and to investigate the spatial variability of eddy covariance fluxes measured above the surface of a feedlot using an analytical flux footprint analysis. A closed-path EC system was used to measure CH_4, CO_2, and H_2O fluxes. To evaluate the performance of this closed-path system, an open-path EC system was also deployed on the flux tower to measure CO_2 and H_2O exchange. The performance assessment of the closed-path EC system showed that this system was suitable for EC measurements. The frequency attenuations, observed for the closed-path system CO_2 and CH_4 cospectra in this study, are in agreement with results from previous instrument comparison studies. For the water vapor closed-path cospectra, larger attenuations were likely caused by water vapor molecule interaction with the sampling tube walls. Values of R^2 for the relationship between H_2O and CO_2 fluxes, measured by open-path and closed-path systems, were 0.94–0.98, respectively. The closed-path EC system overestimated the CO_2 by approximately 5% and underestimated the latent heat fluxes by about 10% when compared with the open-path system measurements. Measured CH_4 and CO_2 fluxes during the study period from the feedlot averaged 2.63 $\mu mol\, m^{-2}\, s^{-1}$ and 103.8 $\mu mol\, m^{-2}\, s^{-1}$, respectively. Flux values were quite variable during the field experiment and the footprint analysis was useful to interpret flux temporal and spatial variation. This study shows indication that consideration of atmospheric stability condition, wind direction and animal movement are important to improve estimates of CH_4 emissions per pen surface or per head of cattle.

1. Introduction

Methane (CH_4) is an important greenhouse gas (GHG) with a global warming potential 28 times greater than CO_2 over a 100-year period (IPCC, 2014). Methane, originating from microbial fermentation in the digestive system of ruminants (enteric fermentation) and manure management, accounts for approximately 30% of the total anthropogenic CH_4 emissions in the United States (USEPA, 2015). Accurate measurements of CH_4 from animal production systems are crucial for reducing uncertainties in national GHG inventories and evaluating mitigation strategies to reduce GHG emissions from agriculture.

Chamber and tracer techniques are often used to measure emissions from livestock. These techniques are useful in comparison studies aiming to evaluate the effect of different diets and mitigation strategies to minimize GHG emissions (Makkar and Vercoe, 2007). However, chambers and tracer techniques are intrusive. They can alter typical animal behavior, management conditions, and gas emission rates. In addition, their application is constrained to a limited number of animals increasing measurement uncertainties (Harper et al., 2011).

Micrometeorological approaches have also been used to estimate GHG emissions from livestock production systems and offer some advantages compared to chamber and tracer techniques (Bai et al., 2015; Baum et al., 2008; Flesch et al., 2007; Laubach, 2010; Laubach et al., 2013). For instance, micrometeorological methods are non-intrusive and integrate flux measurements from larger areas and from a larger number of animals in their natural environ-

* Corresponding author.
E-mail address: esantos@ksu.edu (E.A. Santos).

http://dx.doi.org/10.1016/j.agrformet.2016.09.001
0168-1923/

ment, reducing uncertainties in the fluxes caused by small sample sizes and changes in animal behavior (Harper et al., 2011; McGinn, 2013).

The eddy covariance (EC) technique is considered the most direct micrometeorological method to measure gas exchanges between the land and the atmosphere (Baldocchi, 2003; Dabberdt et al., 1993). EC requires fast response sensors (typically 10–20 Hz sampling rate) to capture fluxes measured by small turbulent eddies. Recent advances in optical sensors have allowed the development of fast response sensors capable of measuring other trace gases, such as CH_4, nitrous oxide (N_2O), and ammonia (NH_3), at a rate suitable for EC measurements (Detto et al., 2011; McDermitt et al., 2011; Peltola et al., 2013; Sun et al., 2015). The EC approach has been used to measure gas exchange from different surfaces, including: agricultural sites (Abraha et al., 2015; Baker and Griffis, 2005), urban plots (Feigenwinter et al., 2012; Velasco et al., 2005), landfills (McDermitt et al., 2013), and bodies of water (Nordbo et al., 2011; Norris et al., 2012). Recent studies have also applied the EC technique to estimate CH_4 emissions from grazing animals (Dengel et al., 2011; Felber et al., 2015).

The EC technique has been applied to measure gas exchange from beef cattle feedlots and the atmosphere (Baum et al., 2008; Sun et al., 2015). Whole farm emission measurements can be useful to improve current modeling approach uncertainties (Crosson et al., 2011). One of the basic assumptions of the EC technique is that measurements are taken above an extensive and homogeneous source area. In feedlots, fluxes measured using the EC approach integrate contributions from different surfaces, such as: pens, roads and alleys, which will influence the flux magnitudes (Baum et al., 2008). Flux footprint analyzes have been used to interpret flux variation in animal production systems and to investigate how changes in the underlying source surface affect flux measurements (Baum et al., 2008; Dengel et al., 2011; Sun et al., 2015). Baum et al. (2008) applied the eddy covariance technique to measure carbon dioxide (CO_2) and water vapor fluxes from a commercial beef cattle feedlot in Kansas. They utilized an analytical footprint model to determine the contributions of non-pen surfaces to the EC flux. They found alleys and roads contribute to 2 and 10% of the total flux, respectively. They also reported that the effect of these surfaces on the fluxes varied depending on the wind direction. More recently, Sun et al. (2015) used the EC approach to measure NH_3 fluxes in a beef cattle feedlot in Colorado. They were able to identify in their two-week measurement that the diel variation in the NH_3 flux was also influenced by the flux footprint.

Most of the CH_4 emission measurements from ruminants using micrometeorological techniques are restricted to short field campaigns ranging from a few days to weeks. Long-term studies are necessary to investigate how changes in environmental conditions affect GHG fluxes from livestock production systems and to reduce the uncertainties of current GHG inventories and emission factors. In addition, long-term studies could bring new insights into the factors affecting the performance of micrometeorological techniques. In this study, we evaluate the performance of a closed-path EC system to measure CH_4 and CO_2 emissions from a commercial beef cattle feedlot during an 8-month period. Few studies have applied the EC technique to quantify gas emissions from a beef cattle feedlot (Baum et al., 2008; Sun et al., 2015) and to our knowledge, this is the first study to utilize the EC technique to estimate long-term CH_4 emissions from a confined animal feeding operation. The main objectives of this study were (i) to assess the performance of a closed-path EC system for measuring CH_4, CO_2, and water vapor (H_2O) fluxes in a beef cattle feedlot against a well-established open-path gas analyzer, and (ii) to investigate the spatial variability of EC fluxes measured above the surface of a beef cattle feedlot using an analytical flux footprint analysis.

2. Material and methods

2.1. Site description

The field experiment was carried out in a commercial beef cattle feedlot in western Kansas from August 2013 to May 2014. This feedlot has a near rectangular shape with a total pen surface of approximately 59 ha surrounded by agricultural fields. The feedlot has the capacity to hold 60,000 head of cattle and was near full capacity (~58,000) during the experiment. The experimental site is on a near flat terrain (slope <5%) and located in one of the windiest regions of the United States (National Climatic Data Center, 2015), making this site ideal to evaluate micrometeorological methods.

2.2. Flux measurements

Fluxes of CH_4, CO_2, latent heat, and sensible heat were measured using the EC technique. Wind velocity, three orthogonal components, and temperature were measured using a sonic anemometer (CSAT3, Campbell Sci., Logan, UT). A wavelength-scanned cavity ring-down spectroscopy closed-path gas analyzer (G2311-f, Picarro Inc., Santa Clara, CA) was used to measure CH_4, CO_2 and H_2O concentrations. To evaluate the performance of the closed-path EC system, a well-established open-path gas analyzer (LI-7500, LI-COR, Lincoln, NE) was also deployed on the flux tower to measure CO_2 and H_2O concentrations.

The closed-path analyzer air intake consisted of a rain diverter connected to an inline filter (Polypropylene/polyethylene 10 μm membrane, Pall Corporation, AnnArbor, MI) and was positioned at 8 cm from the sonic anemometer. The air was drawn from the intake through a 7-m long high density polyethylene tube with an inner diameter of 5.3 mm and then to a second filter (Acrodisc Gelman 1 μm, PTFE membrane, Pall corporation), which was connected to the closed-path analyzer inlet. The feedlot is a very dusty environment, so the use of two filters in series was necessary to prevent clogging of the analyzer's internal filter by particulate material. A vacuum pump (MD 4 NT, Vacuubrand GmbH, Wertheim, Germany) and the analyzer internal mass flow controller kept the flow rate in the sampling line at 5 L min^{-1}. The sampling line was heated using a pipe heating cable and covered with pipe insulation material to lower the relative humidity within the sampling tube and minimize the adsorption of water by the tube walls. Field calibrations were performed in two-week intervals using certified calibration tanks (Tank 1: CH_4 = 1.9 ppm and CO_2 = 350.1 ppm, and Tank 2: CH_4 = 4 ppm and CO_2 = 450.3 ppm, ±1% accuracy, Matheson, Joliet, IL).

The sonic anemometer, closed-path analyzer air inlet, and open-path analyzer were setup on a tower at approximately 5 m above the ground. The tower was mounted on the top of a flatbed trailer at the northern edge of the feedlot. The instrumentation setup location was chosen to maximize air flow over the source area within the feedlot and to maximize the distance between the tower and buildings at the south side of the feedlot that could disturb the air flow. The open-path analyzer was set up with a slight angle from the vertical (~15°) to minimize the accumulation of rain droplets on the analyzer windows after rain events. To minimize synchronization errors among the instruments, the signals of the sonic anemometer, open-path and closed-path gas analyzers were recorded at 10 Hz by a single datalogger (CR1000, Campbell Sci.). The sensors and the datalogger were connected using synchronous devices for measurement (SDM, Campbell Sci) cables for sonic anemometer and open-path analyzer and a serial (RS232) cable for the closed-path analyzer.

2.3. Flux calculations

The high-frequency raw data files were converted into half-hour files using Matlab (version 8.3.0.532, The Mathworks Inc., Natick, MA) functions. These functions were also used to check the consistency of time stamps and to apply the calibration corrections, obtained during field calibrations, to the closed-path analyzer raw signals.

The half-hour high frequency data were then analyzed using the EC package software EddyPro (v. 6.0, Licor). Spikes in the data time series were eliminated following the methodology proposed by Vickers and Mahrt (1997). Averages, covariances, and other statistics were then calculated for 30-min intervals. The block average method was used for calculating turbulent fluctuations and the double rotation method was used to nullify the average cross-stream and components of the wind velocity (Wilczak et al., 2001).

2.3.1. Time lag compensation

Time lags among sonic anemometer and gas analyzer signals arise due to several reasons, such as spatial separation between wind and gas analyzers, as well as differences in computation and digitalization of electronic signals (Aubinet et al., 2012). In addition, in closed-path systems the travelling time of air parcels through the sampling tube and the interaction between gases and tube walls cause gas concentrations to always be measured with a certain delay with respect to the wind velocity measurements. Determining the time lags correctly is an important step of flux calculations as it prevents flux underestimation (Moravek et al., 2013). In our study, compensations for time lags were performed using the covariance maximization method (Fan et al., 1990). For the closed-path EC system, these time lags were determined within a plausible search window. The determination of the plausibility of the time lags is particularly important for low flux conditions when the measured signals contain a large amount of noise leading in some cases to physically unrealistic values of time lag (Detto et al., 2011). The plausibility window was determined by the Eddy Pro software in a preprocessing step that statistically determined the time lags for the closed-path system and their range of variation. Considering the dependence between the water vapor time lags and the relative humidity, the nominal time lags and plausibility windows are determined for different relative humidity classes.

2.3.2. Air density corrections

Fluctuations in temperature and water vapor in the air lead to fluctuations in trace gas concentrations that are not associated with the turbulent transport of the trace gas of interest. Thus, the use of appropriate density corrections is necessary for correct flux computations. For the open-path analyzer, fluxes of CO_2 ($\overline{F_c}$) and H_2O ($\overline{F_v}$) were corrected using the method proposed by Webb et al. (1980), given by:

$$\overline{F_c} = \overline{w'\rho_c'} + \mu_m(\overline{\rho_c}/\overline{\rho}_d)\overline{w'\rho_v'} + (1+\mu_m\sigma)(\overline{\rho_c}/\bar{\theta})\overline{w'\theta'} \quad (1)$$

$$F_v = (1+\mu_m\sigma)[\overline{w'\rho_v'} + (\overline{\rho_v}/\bar{\theta})\overline{w'\theta'}] \quad (2)$$

where w is the vertical wind velocity, ρ is the molar density, the subscripts c, d and v denote: CO_2, dry air and water vapor, respectively; $\mu_m = m_d/m_v$ is the ratio of molar masses of dry air and water vapor; and $\sigma = \overline{\rho_v}/\overline{\rho_d}$ and θ is the potential temperature. Overbars represent the mean and the prime symbols are the departure from the mean.

The closed-path analyzer converts CO_2 and CH_4 mole fractions to mixing ratios, using high frequency measurements of H_2O mixing ratio in the air and an internal algorithm (Chen et al., 2010), which eliminates the need for density corrections. This approach was evaluated as described in Section 3.2.

2.3.3. Spectral corrections

Frequency losses in EC systems are caused by different factors including: inadequate sampling frequency by sensors, sensor separation, and finite sampling duration. In closed-path systems, the existence of sampling tubes and filters, and the residence time in the sampling cell are major causes of spectral attenuation and flux underestimation (Aubinet et al., 2012). Low frequency losses were corrected following the method proposed by Moncrieff et al. (2005). The analytical method proposed by Moncrieff et al. (1997) was used to correct high-frequency losses by the open-path analyzer. For the closed-path system, we applied the spectral correction procedure proposed by Horst (1997), given by:

$$(\overline{w's'})_m/(\overline{w's'})_t = \frac{1}{1+(2\pi n_m \tau_c \bar{u}/z)^{\alpha}} \quad (3)$$

where $(\overline{w's'})_m$ is measured scalar flux or the covariance between w and the scalar concentration s, $(\overline{w's'})_t$ is the un-attenuated scalar flux or expected covariance between w and s, $\bar{u}$ is the average horizontal wind speed at the measurement height z, τ_c is the characteristic time constant of the EC system, α is a stability dependent constant ($\alpha = 7/8$ for neutral and unstable stratification, $z/L \leq 0$, and $\alpha = 1$ for stable stratification, $z/L > 0$), L is the Obukhov length, and n_m is the dimensionless frequency at which the logarithmic cospectrum attains its maximum value. Values of n_m for different conditions of atmospheric stability were estimated using the parameterization proposed by Horst (1997). The time constant τ_c is a function of the transfer function cut-off frequency, which was determined following Ibrom et al. (2007).

2.4. Flux footprint calculation

The upwind distance from the flux tower for a given fraction of the total flux was estimated using the analytical footprint model proposed by Kormann and Meixner (2001). This model is based on the solution of the two-dimensional advection and power law profiles of mean horizontal wind velocity and eddy diffusivity. This simple analytical model is numerically robust and has a reasonable computational time when applied to long-term datasets, as in our study. In addition, the Kormann and Meixner (2001) footprint model has shown good agreement with estimates provided by Lagrangian Stochastic models (Kljun et al., 2003). Following Kormann and Meixner (2001), the cross-wind integrated flux (F_x) at the downwind distance ($x > 0$) from the flux tower is given by:

$$F_x = \frac{1}{\Gamma(\mu)}\frac{\xi^{\mu}}{x^{1+\mu}}e^{-\xi/x} \quad (4)$$

where ξ is a flux length scale, μ is a dimensionless model constant and $\Gamma(\mu)$ is the gamma function. In this study, Eq. (4) was used to estimate x for which the cumulative F_x equals the fraction of the flux contribution of interest (e.g. 70%). The upwind distance, x was calculated for each half hour and combined with wind direction values to assist with the interpretation of the temporal and spatial variabilities of fluxes at the feedlot.

The flux length scale ξ is given by:

$$\xi = \frac{Uz^r}{r^2\kappa} \quad (5)$$

where U and κ are proportionality constants in the power-law profile of the wind velocity and r is the so-called shape factor. The calculation of ξ was performed following the procedure described by Kormann and Meixner (2001) that requires the use of wind velocity, the Obukhov length and the displacement height. The displacement height was determined to be 0.65 m and was calculated using the formulation for sparse plant canopies applied by Baum et al. (2008) in a feedlot study.

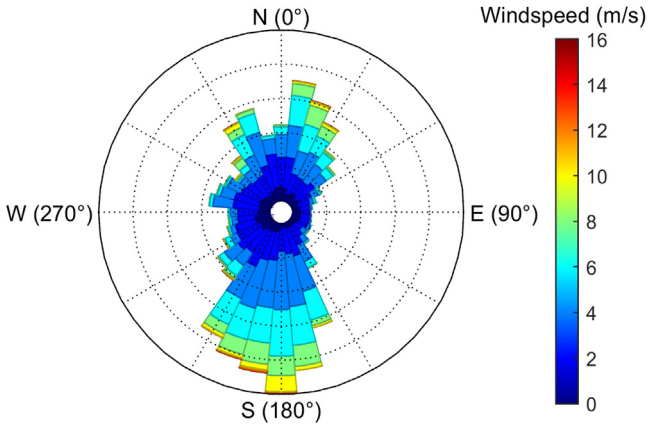

Fig. 1. Frequency distribution of wind direction (North = 0°, East = 90°) and average wind speed during the experimental period.

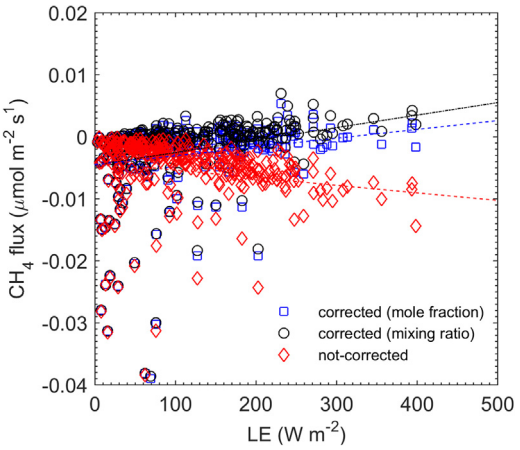

Fig. 2. Relationship between the latent heat flux (LE) and corrected and uncorrected CH_4 fluxes for air density effects. The air density effects were corrected using the close-path analyzer internal algorithm to estimate the CH_4 mixing ratio (circles) and the method proposed by Burba et al. (2012) to correct fluxes calculated using the mole fraction (squares). The non-corrected values are represented by the diamond symbol. Dashed lines represent regression lines for uncorrected fluxes (red line), corrected using the closed-path internal algorithm (black line) and calculated using the mole fraction (blue line). For these analyzes, only small CH_4 fluxes associated with northerly wind directions were selected. (For interpretation of the references to colour in this figure legend, the reader is referred to the web version of this article.)

3. Results and discussion

3.1. Flux data quality control and atmospheric conditions

During the experimental period, power outages and instrument malfunction resulted in the loss of 5% of the 30-min data. Approximately, 4% of open-path system data were excluded due to the accumulation of dust particles and water on the open-path analyzer windows. Regular cleaning of the open-path system window may have limited the data gap.

The remaining half-hourly flux data were screened using the quality control protocol developed by Foken et al. (2004) to test for the development of turbulence and steady state conditions suitable for flux measurements. Using this system, each half-hour period was assigned a quality grade ranging from 1 (best) to 9 (poorest). Foken et al. (2004) recommended the use of flag values smaller than 7 for continuously running EC systems. In our study, we used a slightly stricter criterion excluding flux values associated with quality flags greater than 5 as well as when more than 10% of data points were missing for a given 30-min interval. By using this criterion, 12, 22, and 19% of half-hourly fluxes of CO_2, CH_4, and H_2O, respectively, for the closed-path EC system were excluded from our analysis. The same criterion removed approximately 13% of CO_2 and H_2O half hourly flux data measured by the open-path EC system.

The time lag values for CO_2 and CH_4 were very similar and ranged from 4.5 s to 4.7 s. The small variation in time lag values shows that the flow rate in the closed-path system sampling line was quite constant. For the water vapor, the average time lag was 5.3 s. The greater lag time for H_2O of 5.3 s implies interaction of H_2O with the sampling tube walls.

The average horizontal wind velocity during the experimental period was 4.9 m/s, with prevailing southerly winds greater than 5 m/s being observed in 40% of the time intervals (Fig. 1). The atmospheric stability conditions at the feedlot during the study period were near neutral ($|L| > 100$), unstable ($-100 < L < 0$), and stable ($0 < L < 100$) for 54, 26, and 19% of the time periods, respectively. These prevailing near-neutral conditions at the experimental site are due to the high horizontal wind speeds, low surface heating during the winter months, and the presence of urine and fecal matter on the pen surface, keeping the pen surfaces wet, even during dry and hot days (Baum et al., 2008).

3.2. Density corrections

The closed-path analyzer outputs the gas concentrations for CO_2 and CH_4 in molar density and mixing ratios (χ, mole gas per mole dry air). Molar density values of CO_2 and CH_4 (ρ_m) are converted into mixing ratios of CO_2 (χ_c) and CH_4 (χ_m) using high frequency measurements of water vapor mixing ratio and the following quadratic polynomial functions (Chen et al., 2010):

$$\frac{\rho_c}{\chi_c} = 1 + a\chi_v + b\chi_v^2 \quad (6)$$

$$\frac{\rho_m}{\chi_m} = 1 + c\chi_v + d\chi_v^2 \quad (7)$$

where χ_v is the water vapor mixing ratio reported by the closed-path analyzer at 10 Hz, $a = -0.012$, $b = -2.674 \times 10^{-4}$, $c = -0.00982$, and $d = -2.393 \times 10^{-4}$ are adjusted coefficients for Eqs. (6) and (7), derived from laboratory experiments.

The use of mixing ratios, obtained from Eqs. (6) and (7), for flux calculations theoretically eliminates the need for density corrections for the closed-path analyzer flux calculations. To evaluate the performance of this approach, we applied the procedure proposed by Burba et al. (2012) to correct fluxes calculated using molar densities given by the closed-path analyzer. The effects of water vapor and temperature fluctuations on trace gas fluxes are expected to be proportionally higher when the magnitude of the trace gas flux of interest is low and when the latent heat flux is high (Eq. (1)). For our closed-path system, with a relatively long sampling tube and a temperature-controlled sampling cell, the effect of temperature fluctuations on flux measurements is expected to be negligible. For this analysis, we selected periods in which the area sampled by the flux tower was located outside the feedlot, so that density corrections are expected be large with respect to the CH_4 fluxes.

The relationships between the latent heat flux and CH_4 fluxes, corrected and uncorrected for density effects, are shown in Fig. 2. The non-density corrected CH_4 fluxes became more negative as the magnitude of latent heat flux increased. This apparent CH_4 uptake by the surface is a result of fluctuations in CH_4 concentration caused by fluctuations in air humidity that are not associated with the turbulent transport. Thus, density corrections were applied to the CH_4 fluxes. The average CH_4 fluxes were -0.0055 μmol m^{-2} s^{-1} for non-density corrected fluxes, and equal to -0.0028 μmol m^{-2} s^{-1} and -0.0023 μmol m^{-2} s^{-1} for corrected fluxes following Burba et al. (2012) and the analyzer reported mixing ratio (Chen et al., 2010), respectively. A *t*-test showed that the slopes for the relationships between latent heat and methane fluxes (Fig. 2), corrected using the

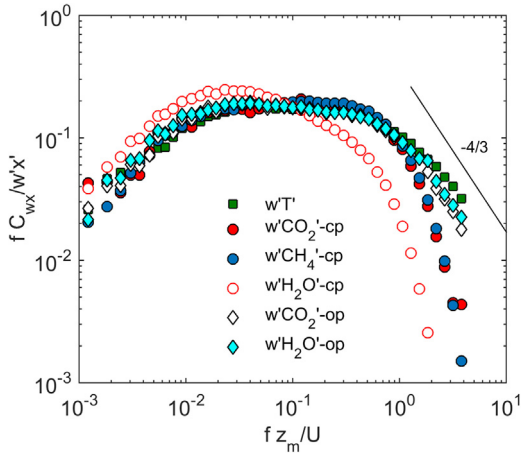

Fig. 3. Normalized cospectra of vertical wind velocity (w) with sonic anemometer temperature (T), CO_2, CH_4 and H_2O calculated using half hourly periods from 12 to 15 h during the experimental period. The symbols op and cp denote open-path and closed-path EC systems, respectively, and f is the frequency, z_m is the measurement height and U is the horizontal wind speed.

two density correction methods were not significant at a 5% probability level. This indicates that the use of the analyzer reported mixing ratios eliminates the need of density corrections.

3.3. Spectral corrections

The ensemble-averaged cospectra, computed for midday (12:00–15:00 h) over the entire study period, were used to investigate closed-path and open-path analyzers' frequency responses (Fig. 3). The sensible heat cospectrum was used as a reference since it is expected to closely follow the cospectrum theoretical predictions when measured at a suitable height under well-developed turbulence conditions (Kaimal et al., 1972). Comparisons with the sensible heat, obtained from the sonic anemometer, and CO_2 and H_2O, measured using a well-established open-path analyzer (LI-7500), were used to evaluate the ability of the closed-path system to measure signals at different frequencies responsible for scalar turbulent transport.

The sensible heat flux cospectrum was slightly less negative than the theoretical slope (−4/3) for the inertial subrange (Kaimal et al., 1972), which has also been previously observed (Baum et al., 2008) and confirms that the sensible heat flux cospectrum is a suitable reference to evaluate the flux losses for other gases (Fig. 3). The ensemble-averaged cospectra for all gas species showed different degrees of frequency attenuation at the inertial sub-range. For the closed-path system, the CH_4, CO_2, and H_2O cospectra showed steeper slopes at the higher frequency band (normalized frequency >1) when compared to CO_2 and H_2O cospectra, measured using the open-path EC system. The ensemble-averaged CH_4 cospectrum was noisier than the other gas curves at the higher frequency end. With the exception of the water vapor closed-path system cospectra, the extent of attenuation was minimal at low frequencies, given the good agreement between the curves at the low frequency band.

The frequency attenuations for the close-path system in this study are in agreement with results from previous comparison studies of CH_4 analyzers (Detto et al., 2011; Peltola et al., 2013). High frequency losses are inherent to closed-path systems and caused by the presence of the sampling line and air filters. For the water vapor, more severe attenuations are mostly likely a result of water vapor molecule interaction with the tubing walls. The EC fluxes were corrected for spectral losses using Horst (1997). The averaged spectral correction factors were: 1.17 for the OP analyzer (CO_2 and H_2O), and 1.22 for CH_4, 1.23 for CO_2 from closed-path system, which are close to the range reported in previous studies by Detto et al. (2011) and Haslwanter et al. (2009). However, a much higher spectral correction factor (2.06) was found for the H_2O flux measured using the closed-path system. Our cospectral analysis suggests that the closed-path system was capable of reasonably measuring CO_2 and CH_4 concentrations for the entire spectrum of frequencies.

3.4. Random error uncertainties

Trace gas flux measurements using the EC technique are prone to random uncertainty errors resulting from instrument errors, changes in flux footprint and the stochastic nature of the turbulence (Finkelstein and Sims, 2001). The random uncertainty error was calculated following the approach by Finkelstein and Sims (2001), which estimates variance of the calculated covariance. The results of this analysis were expressed in terms of distribution of the normalized absolute value of flux error following Peltola et al. (2013) for both the open-path and closed-path EC systems (Fig. 4). All distribution curves were skewed to the left and peaked at low values (0.02–0.03) of fractional flux error. Both closed-path and open-path EC systems showed similar random error uncertainty distribution. The cumulative frequency of occurrence is shown on the right panel of Fig. 4. Approximately 85% of the half-hourly flux values had a random error smaller than 7%. These observations further suggest that the closed-path EC system performed well at the feedlot.

3.5. Open-path and closed-path flux comparisons

Fig. 5 shows the comparisons between CO_2 and H_2O fluxes estimated using the closed-path and open-path EC systems. The regression of CO_2 against H_2O (Fig. 5) for closed-path and open-path EC systems gave R^2 values of 0.94 and 0.98, respectively. The closed-path EC system overestimated CO_2 flux by 5% and underestimated latent heat fluxes by 10% when compared with the open-path system measurements (Fig. 5). A paired t-test showed that closed-path and open-path CO_2 fluxes differences were not significant at a 5% probability level, but the same test indicated that the latent heat fluxes measured by open-path and closed-path EC system were statistically different.

The good agreement between the measurements of open-path and closed-path EC systems indicates that the closed-path EC system is suitable to measure fluxes of passive gases, such as CO_2 and CH_4. However, measurements of water vapor fluxes using closed-path EC systems are more challenging. In the present study, we observed strong dampening of the water vapor signal in the closed-path system (Fig. 3). That signal attenuation by the sampling line is likely to be the main reason for flux underestimations. Physical adsorption and desorption of water vapor by dust particles in the short (~50 cm) stainless tubing located upstream of the air filter, as well as within the walls of the sampling tube, and filters were likely to attenuate the high frequency concentration fluctuations. In future studies, the length of the air intake tubing (between rain diverter and air filter) should be shortened to minimize the accumulation of dust and water vapor adsorption in this section of the sampling line. Furthermore, other hydrophobic tubing materials, such as Teflon and Synflex tubing, and other types of air filters (e.g. Vortex air cleaner, Campbell Sci.) could be an option to improve frequency responses for active gases such as NH_3 and H_2O measured by closed-path EC systems.

Considering the underestimation of the latent heat flux by the closed-path EC system, we hereafter used the latent heat flux provided by the open-path EC system to evaluate the temporal and spatial variability of fluxes at the feedlot. Despite these issues with the water vapor flux measurements, our spectral analysis and

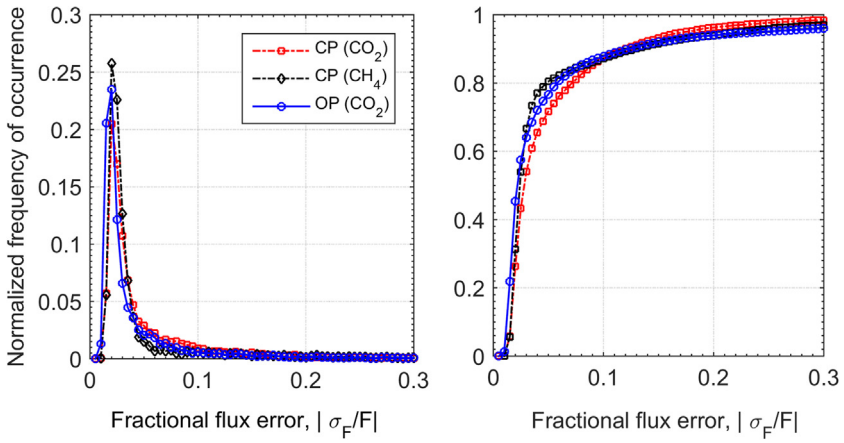

Fig. 4. Distribution curves of absolute value of fractional flux error $\left(|\sigma_F/F|\right)$ (left plot), and cumulative sums of relative frequency of occurrence of respective flux (right plot).

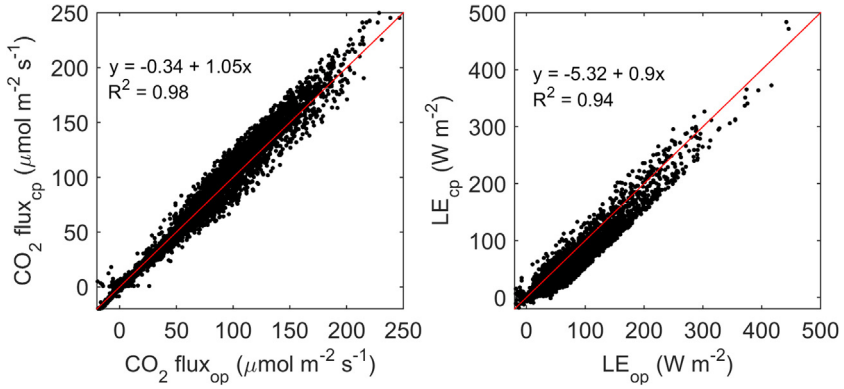

Fig. 5. Comparisons between a) CO_2 (left) and b) latent heat fluxes (LE, right), obtained using two different EC systems: closed-path (cp) and open-path (op) systems. Data on the graphs are half-hourly fluxes from August 2013 to May 2014, which were screened using the method proposed by Foken et al. (2004).

instrument comparisons indicate that the closed-path EC system is suitable for measuring CO_2 and CH_4 fluxes in long-term studies.

3.6. Flux temporal and spatial variability

Half-hourly EC measurements of CH_4, CO_2, latent heat and sensible heat fluxes for the entire experimental period are shown in Fig. 6. The large data gaps in Fig. 6 were the result of equipment malfunctions and power outages. The latent and heat fluxes showed a clear diel and seasonal variation that was related to changes in the availability of solar radiation at the experimental site (Fig. 6 top panels). On the other hand, the fluxes of CH_4 and CO_2 showed large temporal variability (Fig. 6 bottom panels). Higher values of CH_4 and CO_2 fluxes were observed for the months of September and October. The average CH_4 and CO_2 fluxes were equal to 2.63 μmol m^{-2} s^{-1} and 103.8 μmol m^{-2} s^{-1}, respectively, for wind directions ranging from 120° to 240°, assumed to characterize fluxes originated from the feedlot. The magnitude of these fluxes are in agreement with the range of values (1.5–4.6 μmol m^{-2} s^{-1}) reported for CH_4 fluxes by Sun et al. (2015) and (124.6–374.1 μmol m^{-2} s^{-1}) for CO_2 fluxes by Baum et al. (2008) in their respective feedlot studies. In contrast, the average CH_4 and CO_2 fluxes were: 0.032 μmol m^{-2} s^{-1} and 0.63 μmol m^{-2} s^{-1}, respectively, for wind directions ranging from 300° to 60°, which are expected to characterize fluxes originating from the agricultural fields at the north edge of the feedlot. These results show that the feedlot and surrounding fields have very distinct CH_4 and CO_2 source strengths.

The ensemble average half-hourly CO_2 and CH_4 fluxes for wind directions ranging from 120° to 240°, assumed to characterize feedlot fluxes, are shown in Fig. 7. Lower values for CH_4 and CO_2 fluxes were observed at night and in the morning while the higher values were observed during the daytime. Sun et al. (2015) used the EC technique to measure gas emissions from a beef cattle feedlot in Colorado. Their ensemble diel CO_2 and CH_4 fluxes showed smaller variation throughout the day when compared to their composite diel sensible and latent heat fluxes. They reported maximum CH_4 fluxes in the late afternoon and evening. A similar daily pattern for CO_2 fluxes was observed by Baum et al. (2008) for a beef cattle feedlot in Kansas. Our daily ensemble average CO_2 and CH_4 fluxes did not show a distinct peak in the later afternoon and evening as reported in those previous studies. The discrepancies between our results and the ones from previous studies could be related to two factors: 1) differences in management practices among the feedlots, which may affect animal behavior and the temporal dynamics of CO_2 and CH_4 emitted by the cattle; and 2) changes in the source area sampled by the flux tower caused by environmental conditions at the site. To investigate the latter hypothesis, we utilized an analytical footprint model (Kormann and Meixner, 2001), described in Section 2.4, to estimate the upwind distance from the sonic anemometer contributing to 70% of the total fluxes (x_{70}), following previous feedlot studies (Baum et al., 2008; Sun et al., 2015).

The estimated values for x_{70} for day and night periods are shown in Fig. 8. This average distance was 199 m and 352 m for the day and nighttime, respectively. These differences in x_{70} between day and night can be explained by the conditions of atmospheric sta-

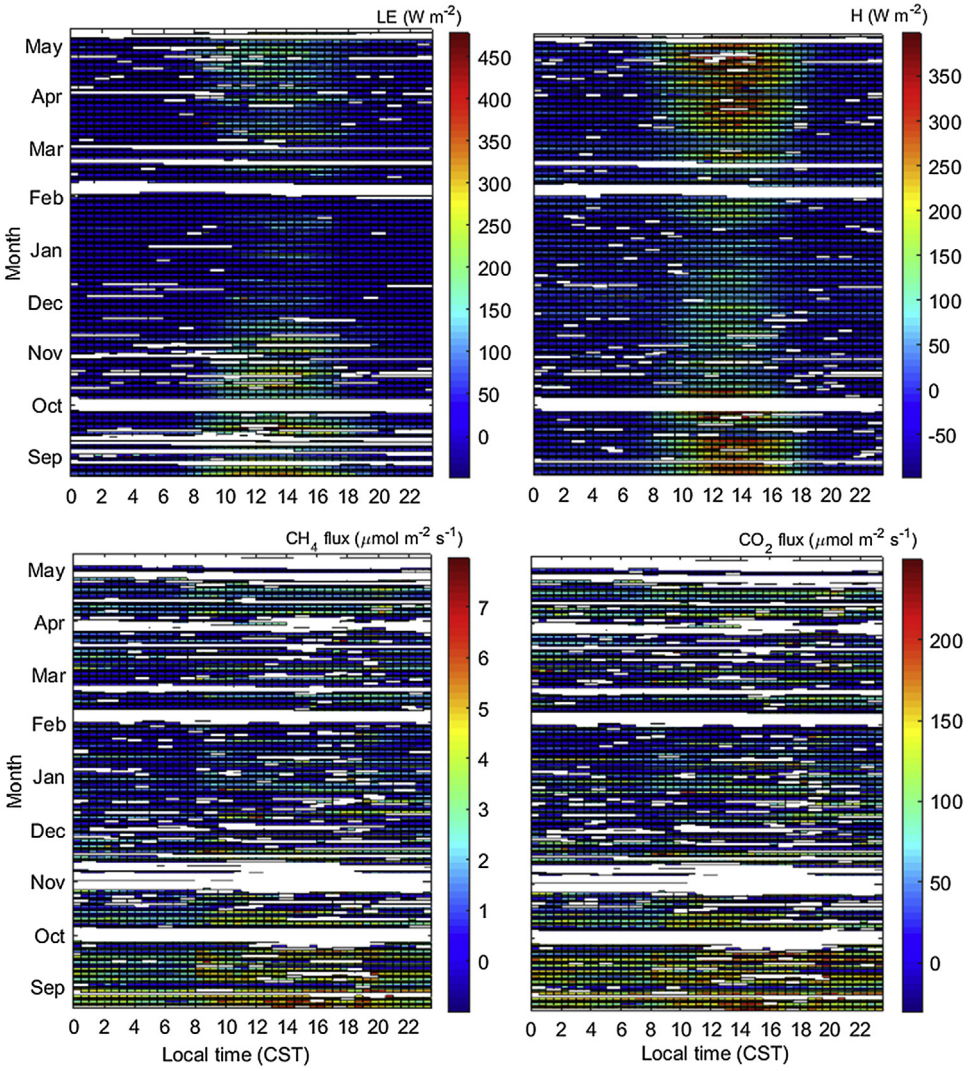

Fig. 6. Diurnal and seasonal variation of CH_4 flux (top left), CO_2 (top right), latent heat (LE) (bottom left), and sensible heat (bottom right) fluxes during the experimental period.

bility. Under stable atmospheric conditions, often common during the nighttime, the flux footprint stretches over a large distance. In contrast, during daytime, solar radiation warms the surface of the feedlot making the atmosphere unstable and convective, resulting in upward motion of scalars that also travel over a short distance (Eugster and Merbold, 2015).

The spatial variation of scalar fluxes was investigated using polar plots of wind direction and footprint distance, expressed by x_{70}, and by grouping scalar fluxes into classes with different magnitudes. All scalar fluxes showed a similar spatial pattern (Fig. 9). In general, higher latent and sensible heat fluxes were associated with x_{70} smaller than 300 m. These higher fluxes were observed during the daytime under convective conditions. Methane and CO_2 fluxes showed a similar spatial variability, with maximum values of fluxes observed for $x_{70} \approx 200$ m and southerly winds. As the wind shifted to eastern and western sectors, flux magnitude tended to decrease, which is explained by the increase of contributions from areas outside the feedlot to eddy fluxes. Higher CO_2 and CH_4 fluxes on the southwest side were likely due to emissions from a manure storage lagoon located at the west side of the feedlot.

Furthermore, as x_{70} increases CO_2 and CH_4 fluxes are more likely to be diluted by non-emitting surfaces within the feedlot. Approximately 28% of the feedlot area is composed of alleys and roads that are used for cattle movement and feed delivery. These sections of the feedlot are expected to have negligible CO_2 and CH_4 emissions, given that animal metabolic processes were the main source of CO_2 and CH_4 at the feedlot. Fluxes that originated from areas further from the tower were likely to be diluted by those surfaces. Baum et al. (2008) combined estimates given by a one-dimensional analytical footprint model and the map with pens and non-pen surfaces, to investigate the impact of changes in the flux tower footprint on their CO_2 flux EC measurements. They found similar effects of non-pen surfaces on the flux calculation. Their raw CO2 fluxes typically increased by 11% when the bias caused by non-emitting surfaces (roads and alleys) was removed from their raw flux measurements. However, under easterly wind conditions, their correction factor was as much as 31% of the raw fluxes due to a larger proportion of roads and alleys in the flux footprint.

To investigate the variability of the CH_4 fluxes within the pens, we screened the CH_4 flux data based on x_{70} (<150 m) and wind direction (175° < wind dir. > 195°). By using this screening criterion, we ensured that most of the contributions to the total CH_4 flux originated from the two pens closest to the flux tower, minimizing the dilution effects from non-emitting surfaces on the CH_4 fluxes. However, results from this analysis still show large variation in fluxes values, with CH_4 flux values ranging from 0.82 to 6.2 μmol m^{-2} s^{-1}

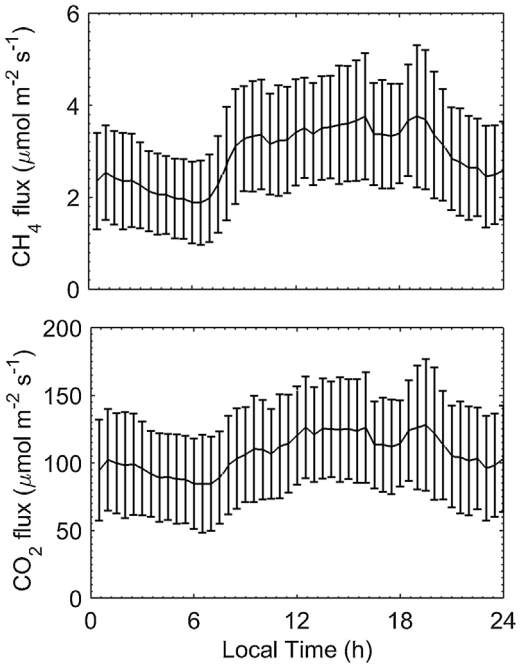

Fig. 7. Daily ensemble average CO_2 and CH_4 fluxes at the study site. Half-hourly fluxes were averaged from August 2013 to May 2014 and screening the data for wind directions ranging from 120° to 240° to include gas emissions originating mostly from the feedlot surface.

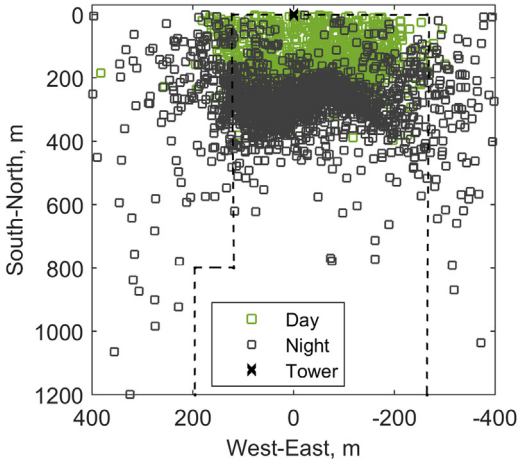

Fig. 8. Upwind distance from the flux tower contributing to 70% of total flux, estimated using an analytical footprint analysis (Kormann and Meixner, 2001) during day time and night time. Only half hourly periods with wind directions ranging from 90° to 270° were included in this analysis. The dotted line indicates the boundary of the feedlot.

(Fig. 10). Several factors could have affected the variability of CH_4 fluxes within the pens, such as: 1) changes in stocking rate in the pens, 2) variations in animal diet, 3) increase in CH_4 production in the pen surface by soil microbes during wet periods and 4) changes in animal position. In this feedlot there was a small reduction in the stocking rate (10–15%) during the winter months (*feedlot manager, personal communication*) and animals from some pens were also replaced, which could account for some long-term flux variability. However, there were no major changes in nutrient content of the diet (data not shown). During the dry cold season, the CH_4 emissions from pen surfaces are expected to be small in comparison with animal emissions. Changes in animal position seems to be the major reason for the short-term CH_4 flux variability in this study.

Animal movement imposes additional challenges to EC measurements of CH_4 emissions from ruminants by creating

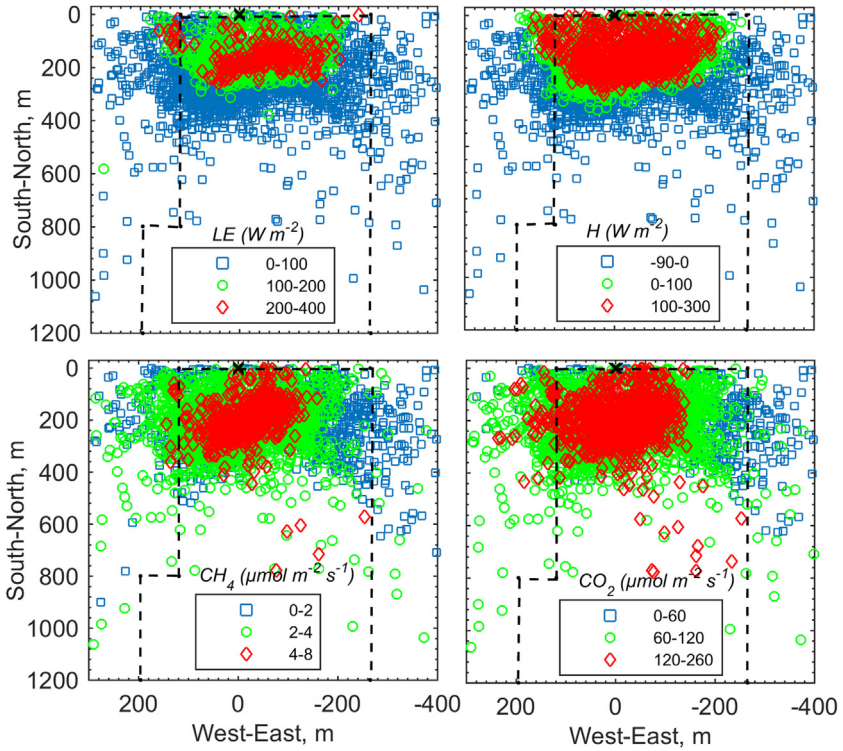

Fig. 9. Spatial distribution of 30 min latent heat (LE), sensible heat (H), CH_4 and CO_2 fluxes in the feedlot during the experimental period. The flux data associated with the footprint distance contributing to 70% of the total flux (Kormann and Meixner, 2001) and wind direction values were grouped in different classes of flux values to investigate the spatial variability of fluxes.

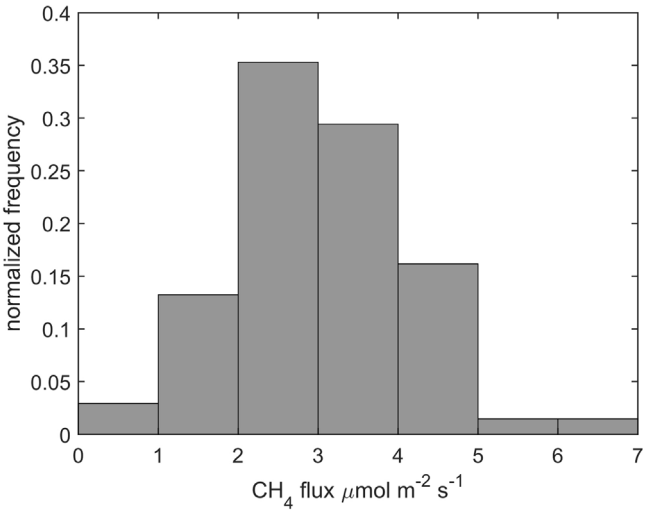

Fig. 10. Frequency distribution of the CH_4 fluxes obtained from pens closer to the flux tower. CH_4 fluxes displayed in this graph were associated with the footprint distance contributing to 70% of the total flux (Kormann and Meixner, 2001) and wind direction values raging from 165° to 205° to minimize the effect road, alleys and other non-emitting surfaces on CH_4 fluxes.

heterogeneities in the source surface and uncertainties in flux measurements. The effect of animal movement in free grazing systems on CH_4 flux measurements has been investigated in recent studies (Baldocchi et al., 2012; Dengel et al., 2011; Felber et al., 2015; Laubach et al., 2013; McGinn et al., 2011). Laubach et al. (2013) measured CH_4 emissions from a herd of cattle using the external tracer technique and two micrometeorological approaches: an inverse dispersion model and a mass balance technique. Their results show that the discrepancies between the mass balance approach and the tracer technique could be explained by uneven animal distribution in the pasture. Felber et al. (2015) used the EC technique combined with a footprint analysis and individual animal position, recorded by GPS units, to estimate CH_4 emissions from dairy cows grazing in paddocks. Their results show that for their grazing system, the inclusion of the position of each animal did not lead to substantial differences in flux estimates per head when compared to similar estimates obtained using only the paddock occupational time. Feedlots have a higher stocking rate than grazing systems which could contribute to a more even flux source area. However, during this experiment, we observed that the cattle in the feedlot gathered near the feed bunks during feeding times leaving the center of the pen nearly empty. In addition, under cold conditions, animals tended to gather in one of the pen corners to minimize heat exchange with the environment. Hence, consideration of animal movement could be important in a confined animal system like a feedlot. In depth investigation of the influence animal positions have on EC measurements is out of the scope of this paper but will be addressed in a manuscript that is under preparation.

4. Conclusions

The performance assessment of the closed-path EC system showed that this system was suitable for EC measurements. The frequency attenuations, observed for the close-path system CO_2 and CH_4 cospectra in this study, are in agreement with results from previous studies. For the water vapor closed-path cospectra, larger attenuations were most likely caused by water vapor molecule interaction with the tubing walls. Values of R^2 for the relationship between H_2O and CO_2 fluxes, measured by open-path and closed-path systems, were 0.94 to 0.98, respectively. The closed-path EC system overestimated the CO_2 by approximately 5% and underestimated the latent heat fluxes by about 10% when compared with the open-path system measurements. In a dusty environment, such as the feedlot in our study, closed-path EC gas analyzers are likely to result in better data retention compared to narrow-band open-path EC analyzers, which are sensitive to the deposition of particulate matter on the sensor window.

Average fluxes of CH_4 and CO_2 from the feedlot were 2.63 μmol m^{-2} s^{-1} and 103.8 μmol m^{-2} s^{-1}, respectively, during the study period. These emission rates were in agreement with other reported studies using micrometeorological methods in feedlots. In general, the flux densities were higher in the pens near the tower under stable conditions, but were lower as the source distance increased under stable conditions, probably due to the dilution effect from road and alleys. However, highly variable flux densities were observed near the tower, which could be related to changes in source strength and homogeneity, caused by for example, animal movement. A manuscript under preparation will evaluate these hypotheses.

This study shows further indication that consideration of atmospheric stability condition, wind direction and animal movement are important to improve the measurement of animal emissions in a feedlot using the EC technique. Additional work is necessary to investigate how heterogeneities in the source area and animal movement affect the flux measurements at the feedlot.

Acknowledgments

We would like to thank our collaborators in the feedlot industry for their assistance with this project and Kansas State University for funding this research project (contribution number 16-284-J from the Kansas Agricultural Experiment Station). We also appreciate the help of Kyle Stropes and Fred Caldwell with the field experiment. We are grateful to the two anonymous reviewers for their contributions to improve this manuscript.

References

Abraha, M., et al., 2015. Evapotranspiration of annual and perennial biofuel crops in a variable climate. GCB Bioenergy 7 (6), 1344–1356.
Aubinet, M., Vesala, T., Papale, D., 2012. Eddy Covariance: a Practical Guide to Measurement and Data Analysis. Springer Science & Business Media.
Bai, M., Flesch, T.K., McGinn, S.M., Chen, D., 2015. A snapshot of greenhouse gas emissions from a cattle feedlot. J. Environ. Qual. 44 (6), 1974–1978.
Baker, J., Griffis, T., 2005. Examining strategies to improve the carbon balance of corn/soybean agriculture using eddy covariance and mass balance techniques. Agric. For. Meteorol. 128 (3), 163–177.
Baldocchi, D., et al., 2012. The challenges of measuring methane fluxes and concentrations over a peatland pasture. Agric. For. Meteorol. 153, 177–187.
Baldocchi, D.D., 2003. Assessing the eddy covariance technique for evaluating carbon dioxide exchange rates of ecosystems: past, present and future. Global Change Biol. 9 (4), 479–492.
Baum, K.A., Ham, J.M., Brunsell, N.A., Coyne, P.I., 2008. Surface boundary layer of cattle feedlots: implications for air emissions measurement. Agric. For. Meteorol. 148 (11), 1882–1893.
Burba, G., et al., 2012. Calculating CO_2 and H_2O eddy covariance fluxes from an enclosed gas analyzer using an instantaneous mixing ratio. Global Change Biol. 18 (1), 385–399.
Chen, H., et al., 2010. High-accuracy continuous airborne measurements of greenhouse gases (CO_2 and CH_4) using the cavity ring-down spectroscopy (CRDS) technique. Atmos. Meas. Tech. 3 (2), 375–386.
Crosson, P., et al., 2011. A review of whole farm systems models of greenhouse gas emissions from beef and dairy cattle production systems. Anim. Feed Sci. Technol. 166-67, 29–45.
Dabberdt, W.F., et al., 1993. Atmosphere-surface exchange measurements. Science 260 (5113), 1472–1481.
Dengel, S., Levy, P.E., Grace, J., Jones, S.K., Skiba, U.M., 2011. Methane emissions from sheep pasture, measured with an open-path eddy covariance system. Global Change Biol. 17 (12), 3524–3533.
Detto, M., Verfaillie, J., Anderson, F., Xu, L., Baldocchi, D., 2011. Comparing laser-based open-and closed-path gas analyzers to measure methane fluxes using the eddy covariance method. Agric. For. Meteorol. 151 (10), 1312–1324.
Eugster, W., Merbold, L., 2015. Eddy covariance for quantifying trace gas fluxes from soils. Soil 1 (1), 187.

Fan, S.M., Wofsy, S.C., Bakwin, P.S., Jacob, D.J., Fitzjarrald, D.R., 1990. Atmosphere-biosphere exchange of CO_2 and O_3 in the central Amazon forest. J. Geophys. Res.—Atmos. 95 (D10), 16851–16864.
Feigenwinter, C., Vogt, R., Christen, A., 2012. Eddy Covariance Measurements over Urban Areas, Eddy Covariance. Springer, pp. 377–397.
Felber, R., Muenger, A., Neftel, A., Ammann, C., 2015. Eddy covariance methane flux measurements over a grazed pasture: effect of cows as moving point sources. Biogeosciences 12 (12), 3925–3940.
Finkelstein, P.L., Sims, P.F., 2001. Sampling error in eddy correlation flux measurements. J. Geophys. Res.—Atmos. 106 (D4), 3503–3509.
Flesch, T.K., Wilson, J.D., Harper, L.A., Todd, R.W., Cole, N.A., 2007. Determining ammonia emissions from a cattle feedlot with an inverse dispersion technique. Agric. For. Meteorol. 144 (1-2), 139–155.
Foken, T., et al., 2004. Post-field Data Quality Control, Handbook of Micrometeorology. Springer, pp. 181–208.
Harper, L.A., Denmead, O.T., Flesch, T.K., 2011. Micrometeorological techniques for measurement of enteric greenhouse gas emissions. Anim. Feed Sci. Technol. 166–67, 227–239.
Haslwanter, A., Hammerle, A., Wohlfahrt, G., 2009. Open-path vs. closed-path eddy covariance measurements of the net ecosystem carbon dioxide and water vapour exchange: a long-term perspective. Agric. For. Meteorol. 149 (2), 291–302.
Horst, T., 1997. A simple formula for attenuation of eddy fluxes measured with first-order-response scalar sensors. Bound.—Layer Meteorol. 82 (2), 219–233.
IPCC, 2014. Climate Change 2014: Synthesis Report. Contribution of Working Groups I, II and III to the Fifth Assessment Report of the Intergovernmental Panel on Climate Change. In: Core Writing Team, Pachauri, R.K., Meyer, L.A. (Eds.). IPCC, Geneva, Switzerland.
Ibrom, A., Dellwik, E., Flyvbjerg, H., Jensen, N.O., Pilegaard, K., 2007. Strong low-pass filtering effects on water vapour flux measurements with closed-path eddy correlation systems. Agric. For. Meteorol. 147 (3-4), 140–156.
Kaimal, J., Wyngaard, J., Izumi, Y., Coté, O., 1972. Spectral characteristics of surface-layer turbulence. Q. J. R. Meteorol. Soc. 98 (417), 563–589.
Kljun, N., Kormann, R., Rotach, M., Meixer, F., 2003. Comparison of the Langrangian footprint. Bound.—Layer Meteorol. 106 (2), 349–355.
Kormann, R., Meixner, F.X., 2001. An analytical footprint model for non-neutral stratification. Bound.—Layer Meteorol. 99 (2), 207–224.
Laubach, J., et al., 2013. Accuracy of micrometeorological techniques for detecting a change in methane emissions from a herd of cattle. Agric. For. Meteorol. 176, 50–63.
Laubach, J., 2010. Testing of a Lagrangian model of dispersion in the surface layer with cattle methane emissions. Agric. For. Meteorol. 150 (11), 1428–1442.
Makkar, H., Vercoe, P., 2007. Measuring Methane Poduction from Ruminants. Springer, Dordrecht, The Netherlands.
McDermitt, D., et al., 2011. A new low-power, open-path instrument for measuring methane flux by eddy covariance. Appl. Phys. B: Lasers Opt. 102 (2), 391–405.
McDermitt, D., Xu, L., Lin, X., Amen, J., Welding, K., 2013. Impact of changes in barometric pressure on landfill methane emission. EGU Gen. Assem. Conf. Abstr., 5435.
McGinn, S.M., et al., 2011. Methane emissions from grazing cattle using point-source dispersion. J. Environ. Qual. 40 (1), 22–27.
McGinn, S.M., 2013. Developments in micrometeorological methods for methane measurements. Animal 7, 386–393.
Moncrieff, J.B., et al., 1997. A system to measure surface fluxes of momentum sensible heat, water vapour and carbon dioxide. J. Hydrol. (Amsterdam) 188–189 (1/4), 589–611.
Moncrieff, J., Clement, R., Finnigan, J., Meyers, T., 2005. Averaging, Detrending, and Filtering of Eddy Covariance Time Series, Handbook of Micrometeorology. Springer, pp. 7–31.
Moravek, A., Trebs, I., Foken, T., 2013. Effect of imprecise lag time and high-frequency attenuation on surface-atmosphere exchange fluxes determined with the relaxed eddy accumulation method. J. Geophys. Res.: Atmos. 118 (17).
National Climatic Data Center, Comparative climatic data publication: wind-average speed (MPH). http://www1.ncdc.noaa.gov/pub/data/ccd-data/wndspd15.dat, 2013. (accessed 31.08.16).
Nordbo, A., et al., 2011. Long-term energy flux measurements and energy balance over a small boreal lake using eddy covariance technique. J. Geophys. Res.: Atmos. 116 (D2), 1984–2012.
Norris, S.J., et al., 2012. Eddy covariance measurements of the sea spray aerosol flux over the open ocean. J. Geophys. Res.: Atmos. 117 (D7), 1984–2012.
Peltola, O., Mammarella, I., Haapanala, S., Burba, G., Vesala, T., 2013. Field intercomparison of four methane gas analyzers suitable for eddy covariance flux measurements. Biogeosciences 10 (6), 3749–3765.
Sun, K., et al., 2015. Open-path eddy covariance measurements of ammonia fluxes from a beef cattle feedlot. Agric. For. Meteorol. 213, 193–202.
USEPA, 2015. U.S. Greenhouse Gas Inverntory Report: 1990–2013. USEPA, Washington, DC.
Velasco, E., Pressley, S., Allwine, E., Westberg, H., Lamb, B., 2005. Measurements of CO_2 fluxes from the Mexico City urban landscape. Atmos. Environ. 39 (38), 7433–7446.
Vickers, D., Mahrt, L., 1997. Quality control and flux sampling problems for tower and aircraft data. J. Atmos. Ocean. Technol. 14 (3), 512–526.
Webb, E., Pearman, G., Leuning, R., 1980. Correction of flux measurements for density effects due to heat and water vapour transfer. Q. J. R. Meteorol. Soc. 106 (447), 85–100.
Wilczak, J.M., Oncley, S.P., Stage, S.A., 2001. Sonic anemometer tilt correction algorithms. Bound.—Layer Meteorol. 99 (1), 127–150.